

# Molecular Simulation Study on the Influence of Dimethylsulfoxide on the Structure of Phospholipid Bilayers

Amadeu K. Sum and Juan J. de Pablo

Department of Chemical and Biological Engineering, University of Wisconsin, Madison, Wisconsin

**ABSTRACT** Molecular dynamics simulations of dipalmitoylphosphatidylcholine (DPPC) lipid bilayer/water systems were performed in the presence of dimethylsulfoxide (DMSO) at 2, 5, 10, and 100 mol % DMSO (lipid-free basis). The equilibrium structure and several dynamic properties were determined for these systems. Results show that DMSO penetrates much deeper into the bilayer than water does. It is also found that DMSO molecules do not interact with the polar groups of the lipid headgroup, but exhibit a preference to remain either directly below the headgroup or in the aqueous phase, which is a consequence of the chemical characteristics of DMSO. As the temperature increases, a higher DMSO concentration is observed in the bilayer side of the interface. The area per headgroup in the presence of DMSO is significantly increased from 66.8 Å<sup>2</sup> for the pure bilayer to as high as 87.0 Å<sup>2</sup> at 10 mol % DMSO at 350 K. DMSO hydrogen-bonds strongly with water and exhibits unfavorable interactions with the polar headgroups of DPPC, thereby inducing a dehydration of the headgroups.

## INTRODUCTION

Dimethylsulfoxide (DMSO) is often used in biology as a cryoprotectant agent. It is used for preservation of enzymes and cells during freezing, and it is also used for perfusion of organs before transplant. Many of the protocols that are followed for cryopreservation of mammalian cells specify that the media used to freeze the cells should contain 10 wt % (2.5 mol %) DMSO (Freshney, 1987). DMSO exhibits significant pharmacological activity, including anti-inflammatory and analgesic effects. It also acts as a muscle relaxant agent, and it enhances cell differentiation and function (Jacob and Herschler, 1986). The widespread use of DMSO has led to numerous studies and hypotheses about its properties and interactions with biological organisms.

Several experimental studies have investigated the structure of model cell membranes (phospholipid bilayers) in the presence of DMSO (Chang and Dea, 2001; Gordeliy et al., 1998; Kiselev et al., 1999; Shashkov et al., 1999; Tristam-Nagle et al., 1998; Yamashita et al., 2000; Yu and Quinn, 1998, 2000). Most of these studies have used x-ray diffraction and differential scanning calorimetry to probe the structure and phase behavior of lipid bilayers over a wide range of DMSO concentrations. Gordeliy et al. (1998) performed x-ray diffraction measurements on lipid bilayers in the presence of DMSO over the entire concentration range (DMSO/water); they characterized the phase behavior and concluded that there is a strong interaction between DMSO and the bilayer surface. Tristam-Nagle et al. (1998) investigated the equilibrium phases and kinetics of a sub-gel phase in dipalmitoylphosphatidylcholine (DPPC) with DMSO, and attributed the changes in the phase behavior of the lipid bilayers to the dehydrating effect caused by DMSO.

Yu and Quinn (1998; 2000) performed x-ray diffraction on bilayers containing up to 50 wt % (18.7 mol %) DMSO and found that the thickness of the bilayer decreases and that the area per headgroup increases. Kiselev et al. (1999) used diffraction, scattering, and calorimetry to determine the influence of DMSO on the structure and phase transitions of DPPC bilayers over the entire DMSO concentration spectrum; their results showed that DMSO molecules do not penetrate the polar headgroup region or its vicinity. Shashkov et al. (1999) used infrared spectroscopy in addition to x-ray and calorimetry to probe the competition between DMSO and water for interactions with the bilayer surface, and found that the resulting dehydration of the lipid bilayer is caused by the strong interaction between DMSO and water. Chang and Dea (2001) used calorimetry to study the effect of DMSO on the phase transitions of lipid bilayers, and concluded that the presence of DMSO affects the solvation of the lipid bilayer. Yamashita et al. (2000) looked at the stability of bilayers at low DMSO concentrations (<30 mol %) and found that the transition temperature from a gel to a liquid-crystalline phase increases with increasing DMSO concentration.

More generally, it is known that DMSO can hydrogen-bond with water (Martin and Hauthal, 1971; Shashkov et al., 1999); it is also believed that DMSO has the ability to replace water and solvate lipid headgroups (Gordeliy et al., 1998; Kiselev et al., 1999; Tristam-Nagle et al., 1998). DMSO is also known to easily permeate membranes (Anchordoguy et al., 1992), a characteristic that may be favored by its hydrophobic groups (two methyl groups). The small size of DMSO and its dual character (hydrophobic and hydrophilic) facilitate interactions with the different environments present in a lipid bilayer system, that is, the aqueous and bilayer regions.

Only two computational studies of DMSO with lipid bilayers have appeared in the literature. The work by Smondyrev and Berkowitz (1999) considered the properties

*Submitted May 27, 2003, and accepted for publication August 27, 2003.*

Address reprint requests to Juan J. de Pablo, Tel.: 608-262-7727; Fax: 608-262-5434; E-mail: depablo@engr.wisc.edu.

© 2003 by the Biophysical Society

0006-3495/03/12/3636/10 \$2.00

of a lipid bilayer in the presence of pure DMSO; their results will be discussed later in this work. The study of Paci and Marchi (1994) examined the transport of a single DMSO molecule through a lipid bilayer. This work provides a detailed analysis of DPPC lipid bilayers in the presence of DMSO over a wide range of concentrations commonly encountered in the preservation of biological systems.

## SIMULATION DETAILS

Molecular dynamics simulations were performed on systems containing a total of 128 dipalmitoylphosphatidylcholine (DPPC) molecules arranged in a bilayer structure (64 molecules on each side) in the presence of water and dimethylsulfoxide (DMSO). Initial configurations for the systems of interest were generated starting from a fully hydrated bilayer and by randomly replacing water molecules with DMSO molecules (Sum et al., 2003). The composition of the systems considered in this work are given in Table 1. At each temperature and composition, the system was allowed to equilibrate for at least 1 ns; equilibrium properties were accumulated over simulations of at least 10 ns. A timestep of 2 fs was used for all simulations with a leapfrog integration algorithm (Allen and Tildesley, 1987). Non-bonded interactions were cut off beyond 9 Å. We have performed our simulations using both a reaction-field correction method ( $\epsilon_{\text{RF}} = 80$ ) (Allen and Tildesley, 1987) and a particle-mesh Ewald method (Essman et al., 1995) for the long-range electrostatic interactions; we do not find significant differences between the results of both approaches in ns-long simulations. Recent comparisons between different long-range correction techniques (reaction-field correction, Ewald summation, switched potentials) commonly used in simulations of biological systems (Faraldo-Gómez et al., 2002; Nina and Simonson, 2002; Norberg and Nilsson, 2000; Tobias, 2001) suggest that the results of reaction-field and Ewald summation simulations of lipid bilayers are equivalent. A more recent publication (Patra et al., 2003) addressed the shortcomings of truncating the electrostatic interactions using a large cutoff (without reaction-field or Ewald summations); this, however, was not the case in this work. The temperature and pressure of the simulation box were kept constant using the weak coupling technique (Berendsen et al., 1984), with correlation times  $\tau_T = 0.2$  ps and  $\tau_P = 2.5$  ps for temperature and pressure, respectively. For constant-pressure simulations, the three

Cartesian directions were independently coupled to an ambient pressure of  $p = 101.3$  kPa with a compressibility  $\kappa = 0.46 \times 10^{-6}$  kPa $^{-1}$ , thereby allowing the area of the bilayer and the distance between the interfaces to fluctuate independently.

The force field employed in our simulations was assembled from various sources: the GROMOS force field (van Gunsteren et al., 1996) was used for the headgroups of DPPC, and for the aliphatic tails the NERD force field (Nath et al., 2001, 1998; Nath and de Pablo, 2000) was employed (note, however, that the force constants corresponding to bond-stretching in the NERD force field were strengthened by two orders of magnitude to be consistent with the GROMOS parameters). The SPC/E model (Berendsen et al., 1987) was adopted for water. For DMSO we used the improved force field developed by Müller-Plathe and co-workers (Bordat et al., 2003).

## RESULTS AND DISCUSSION

The equilibrium thermodynamic properties and structure of various DPPC/water/DMSO systems were calculated over long simulations runs. It is instructive to note that the phase transition temperature from a gel to a liquid crystalline phase for a DPPC/water/DMSO system increases with increasing DMSO concentration (Shashkov et al., 1999). At the DMSO concentrations considered in this work, the experimental phase transition temperatures are approximately 316 K at 2 mol %; 317 K at 5 mol %; 320 K at 10 mol %; and 350 K at 100 mol %. All conditions chosen in this study are above the phase transition temperature and therefore correspond to stable systems in a liquid crystalline phase.

Fig. 1 shows the total and individual component density profiles for each DMSO concentration at 350 K. Three regions can be distinctively identified, corresponding to the bulk aqueous phase, the interface consisting of the lipid headgroups, and the interior of the lipid bilayer. The reference plane ( $z = 0$ ) is the point of lowest density, that is, the region where the lipid tails of opposite sides meet. The region of highest density corresponds to the lipid headgroups that form the interface between the lipid and the aqueous regions. That region of high density correlates well with the position of the phosphorus atoms in the lipid headgroup.

The DMSO density profile exhibits several interesting features at concentrations up to 10 mol %; in the aqueous region, DMSO is well-solvated by water molecules through hydrogen-bonding and it is uniformly distributed. The water and DMSO concentrations decrease through the interface region; the number of water molecules steadily decays to zero, whereas the DMSO concentration reaches a minimum, then peaks at  $\sim |z| = 10\text{--}12$  Å, and decays to a small value inside the bilayer. Note that the dip in the DMSO density profile is located around the maximum phosphorus concentration. This suggests that DMSO interacts unfavorably with the polar headgroups of DPPC, but exhibits favorable

**TABLE 1** Composition of simulated lipid bilayer systems

System	Water	DMSO	DMSO concentration*
DMSO-A	3582	73	8.1 wt %/2.0 mol %
DMSO-B	3472	183	18.6 wt %/5.0 mol %
DMSO-C	3290	365	32.5 wt %/10.0 mol %
DMSO-D	—	1536	100.0 wt %/100.0 mol %

For all cases, 128 DPPC molecules are used.

\*Lipid-free basis.

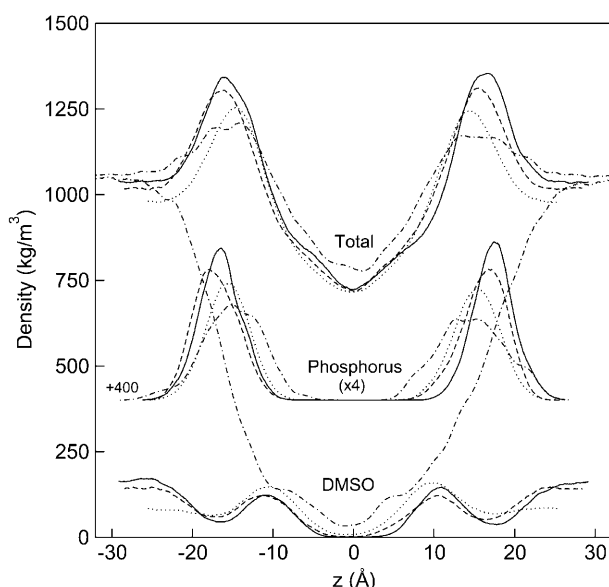


FIGURE 1 Density profiles of fully hydrated DPPC bilayer with DMSO at 350 K: DMSO-A (solid line), DMSO-B (dashed line), DMSO-C (dotted line), and DMSO-D (dot-dashed line). See Table 1 for additional information.

interactions with water in the aqueous region and with the aliphatic part of the lipid. At the highest DMSO concentration considered in this work (10 mol % at 350 K), DMSO can penetrate and diffuse across the bilayer (from side to side). Fig. 2 shows the trajectory of two DMSO molecules over the course of the simulation run at 10 mol % DMSO and 350 K. At the beginning of the simulation, a particular DMSO

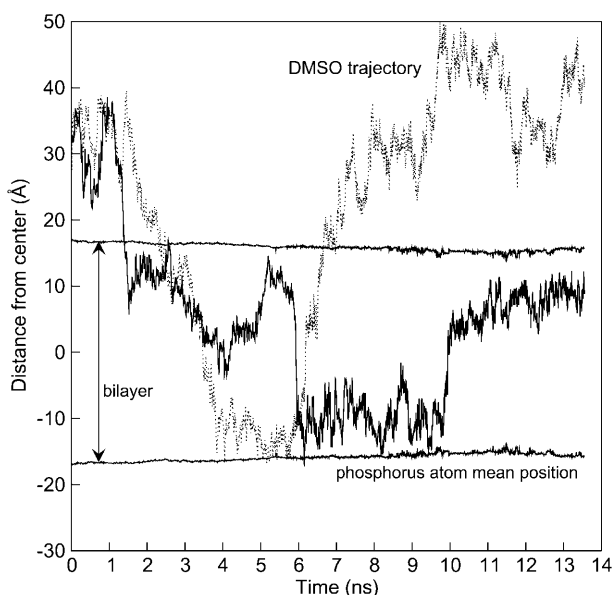


FIGURE 2 Trajectory for two DMSO molecules from the DMSO-C system at 350 K in the DPPC/water/DMSO system. The zero position corresponds to the lipid bilayer center, and the mean position of the phosphorus atoms in each layer is given for reference.

molecule (solid line in Fig. 2) is in the aqueous region, and at  $\sim 1.5$  ns, it crosses the interface. This crossing process occurs within a few picoseconds because of the unfavorable interaction of DMSO with the lipid polar groups. Once this molecule crosses the interface, it diffuses in the bilayer region and remains there for the remainder of the simulation ( $\sim 10$  ns). A second DMSO molecule (dotted line in Fig. 2), also initially in the aqueous region, penetrates and remains in the bilayer for several nanoseconds before it returns to the aqueous phase. It is clear from the trajectories that DMSO has the ability to diffuse from one side of the bilayer to the other. The penetration of DMSO molecules through the interface is an activated process in that DMSO molecules require a substantial amount of energy to overcome the energy barrier (breaking of hydrogen-bond between DMSO and water) and cross the interface from either side. The dual role assumed by DMSO, hydrophobic and hydrophilic, can be explained by its size and functionality: the polar part can hydrogen-bond with water and the methyl groups can interact favorably with the aliphatic lipid tails.

Fig. 1 also shows the density profile for the binary DPPC/DMSO system (without water) at 350 K. In this case, a large number of DMSO molecules penetrate the bilayer; the DMSO concentration decreases from the bulk DMSO region to the middle of the bilayer region, where a steady concentration of DMSO is observed. Because of the hydrophobic nature of DMSO and its favorable interaction with the lipid aliphatic tails, the bilayer structure is deformed—that is, the bilayer interface is not as well-defined as in the case with lower DMSO concentrations. Furthermore, the integrity of the bilayer structure is modified by the lipid

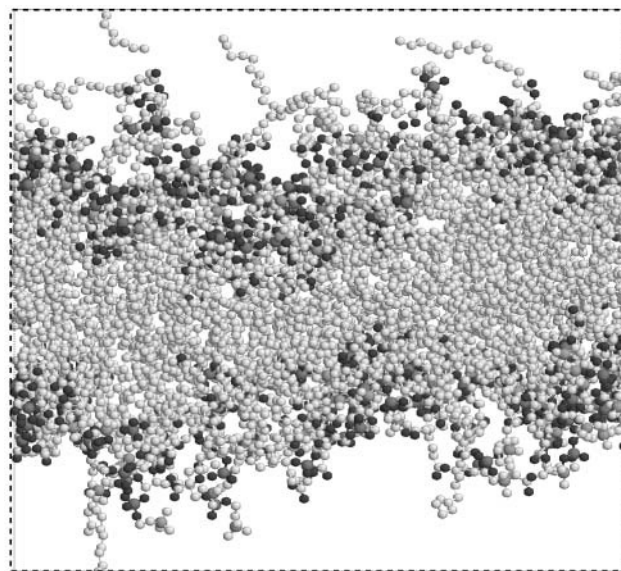


FIGURE 3 Snapshot of the DPPC/DMSO simulation box at 350 K. DMSO molecules have been removed for clarity. Note how some lipid alkyl chains protrude into the DMSO bulk phase.

aliphatic tails dissolving into the DMSO bulk region. This is illustrated in Fig. 3, which shows a snapshot of the lipids in the simulation box (for clarity, DMSO molecules are not shown). Several lipid tails can be seen protruding from the bilayer into the bulk DMSO region. Smondyrev and Berkowitz (1999) have also performed simulations of a lipid bilayer in pure DMSO (a system with 64 DPPC molecules at 323 K and for 2 ns of simulation time); these authors pointed out that only a small number of DMSO molecules are able to penetrate the bilayer region. Note, however, that Smondyrev and Berkowitz used a different force field and performed their calculations at a lower temperature.

For the lipid bilayer system, the potential of mean force (PMF) experienced by DMSO molecules as they move from the aqueous region to the interface and the inside of the lipid bilayer can be directly related to the concentration profile by

$$\text{PMF} = -RT \ln [\rho(z)], \quad (1)$$

where  $\rho$  is the density profile along the normal direction to the interface,  $T$  is the temperature, and  $R$  is the universal gas constant. Simulation results for the bilayer system with 10 mol % DMSO at 350 K indicate that a significant amount of DMSO molecules passes through the interface and penetrates into the bilayer; using this concentration profile (see Fig. 1), the potential of mean force for DMSO was calculated as shown in Fig. 4, which also shows the density profile for DMSO and water as reference for the relative location along the bilayer (the reference point for the potential of mean force,  $\text{PMF} = 0$ , corresponds to DMSO molecules in the aqueous region). The potential of mean force for DMSO increases as it approaches the lipid/water interface; it reaches

a peak, and then decreases slightly until it increases to large values toward the center of the bilayer. Paci and Marchi (1994) attempted to calculate the potential of mean force for a single DMSO molecule through a lipid bilayer by constraining the molecule at different positions along the bilayer. Unfortunately, the results were not conclusive because their calculations were relatively short ( $\sim 300$  ps). These authors did report a change in energy of  $\sim 80$  kJ/mol for transferring a DMSO molecule from the aqueous region to a position well inside the bilayer.

Fig. 5 shows how the local DMSO concentration in the bilayer system changes as a function of temperature. At the lower temperature of 325 K, DMSO tends to concentrate more in the aqueous region than in the bilayer; at 400 K, there is a shift in the relative concentrations, and DMSO is found predominantly in the bilayer. The hydrogen bonds between DMSO and water are favored at low concentrations and low temperatures. At higher temperatures, this hydrogen-bonding becomes weaker, DMSO adopts a more hydrophobic character, and it prefers to interact with the bilayer tails. This change in relative concentration with temperature is a manifestation of the hydrophobic effect, and has been invoked before to explain the toxicity of DMSO in cellular cryopreservation (Anchordoguy et al., 1992, 1991). It should also be pointed out that even though DMSO and water molecules are strongly hydrogen-bonded, there is no indication that water molecules penetrate the bilayer interface; in other words, DMSO is unable to act as a carrier for water into the bilayer. In the process of crossing the bilayer interface, DMSO must release the water molecules to which it is bound, thereby assuming an instantaneous transformation from hydrophilic to hydrophobic. This is also indicated

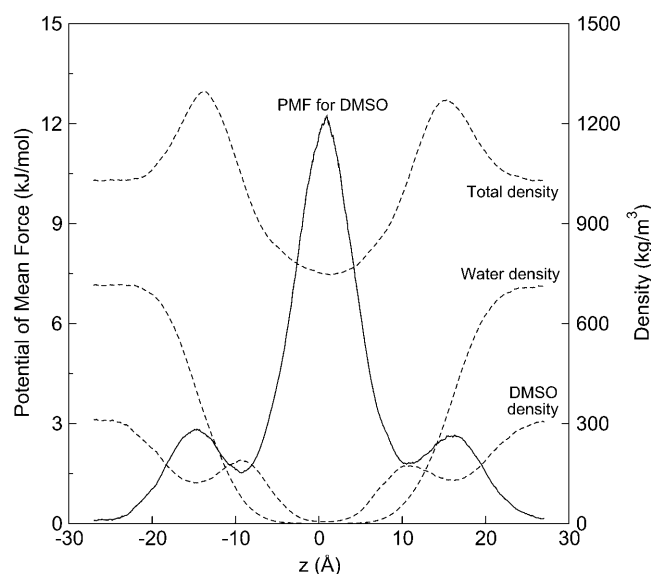


FIGURE 4 Potential of mean force for DMSO calculated from the density profile for the DMSO-C system at 350 K. The solid curve represents the PMF, and the dashed curves are the density profiles.

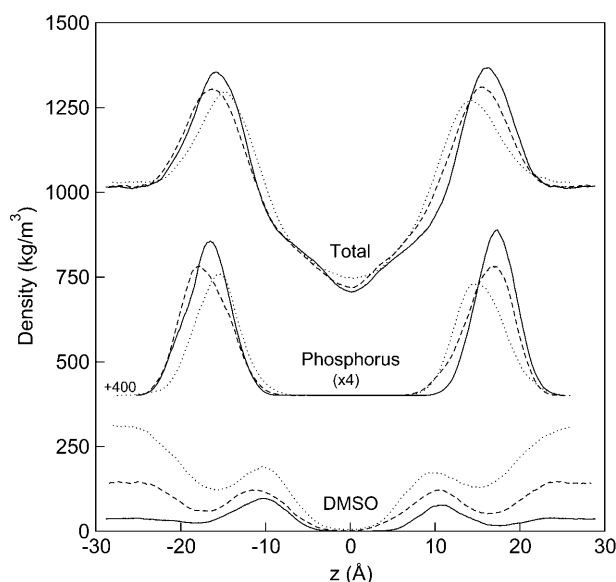


FIGURE 5 Density profiles of the DMSO-B system: 325 K (solid line) and 400 K (dashed line).

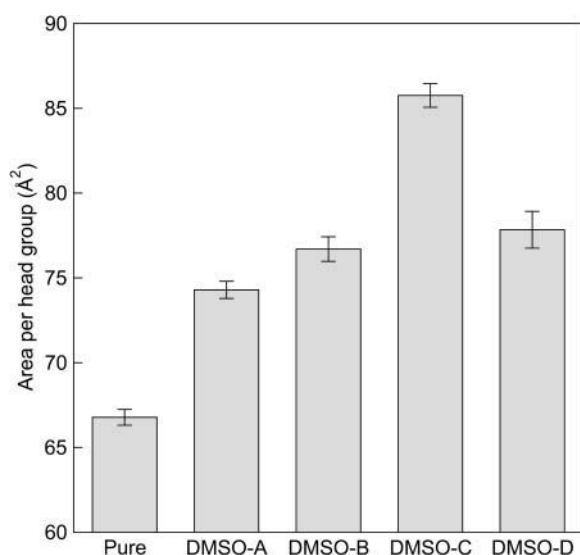
**TABLE 2** Area per headgroup for lipid bilayer with DMSO

System	$T$ (K)	Area ( $\text{\AA}^2$ )
Pure*	325	$64.7 \pm 0.7$
	350	$66.8 \pm 0.5$
	400	$72.2 \pm 0.9$
DMSO-A	350	$71.2 \pm 0.7$
DMSO-B	325	$72.1 \pm 0.7$
	350	$76.7 \pm 0.7$
	400	$86.5 \pm 0.7$
DMSO-C	350	$87.0 \pm 0.7$
DMSO-D	350	$77.3 \pm 2.3$

\*From Sum et al. (2003).

from the fast crossing of DMSO molecules through the interface (see Fig. 2).

Table 2 shows the area per headgroup for the systems considered in this work. Fig. 6 compares these values to those obtained from simulations of pure bilayers at 350 K. Addition of DMSO to the bilayer significantly increases the area per headgroup (area along the bilayer surface divided by the number of lipids per layer, 64 in our case). The area per headgroup increases from  $66.8 \text{ \AA}^2$  in the pure bilayer to  $87.0 \text{ \AA}^2$  in the system with 10 mol % DMSO at 350 K. This increase in area per headgroup can be understood by the fact that DMSO penetrates the bilayer, and resides preferentially in the spaces immediately underneath the headgroups, as seen from the density profiles in Fig. 1. Moreover, since DMSO has a larger molecular volume than water, it expands the distance between the headgroups to penetrate the bilayer; the higher the DMSO concentration, the larger the number of DMSO molecules diffusing through the interface, and the larger the separation distance between the headgroups. The area per headgroup depends strongly on temperature. For the systems with 5 mol % DMSO, the area per headgroup

**FIGURE 6** Area per headgroup of phospholipids in a DPPC bilayer with DMSO at 350 K.

increases from  $72.1$  to  $86.5 \text{ \AA}^2$  between 325 and 400 K. Simulations of DPPC in pure DMSO also reveal a large increase in the area per headgroup ( $77.3 \pm 2.3 \text{ \AA}^2$  at 350 K). Based on x-ray diffraction measurements of a bilayer system with 11 mol % DMSO, Yu and Quinn (1998) have reported an increase in the area per headgroup (unfortunately these changes were not quantified). In contrast to our findings, a previous simulation study (Smodyrev and Berkowitz, 1999) of a lipid bilayer in pure DMSO reported that the area per headgroup ( $60.4 \pm 0.6 \text{ \AA}^2$ ) does not differ appreciably from that of a DPPC/water system ( $61.6 \pm 0.6 \text{ \AA}^2$ )—as noted above, that study was based on a different force field and temperature. Given the consistency with experimental observations, we believe that the model and results presented here provide a more accurate description of DPPC/water/DMSO systems.

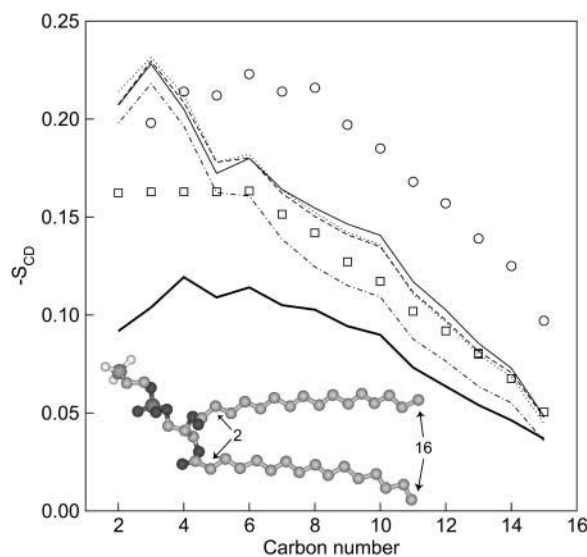
The lipid tail order parameter,  $S_{CD}$  (Tielemann et al., 1997), provides a measure of the alignment of the phospholipid tails in the bilayer. It is given by

$$-S_{CD} = \frac{2}{3}S_{xx} + \frac{1}{3}S_{yy}, \quad (2)$$

$$S_{\alpha\beta} = \langle 3 \cos \Theta_\alpha \cos \Theta_\beta - \delta_{\alpha\beta} \rangle, \quad \alpha, \beta = x, y, z \quad (3)$$

$$\cos \Theta_\alpha = \hat{e}_\alpha \hat{e}_z, \quad (4)$$

where  $\hat{e}_z$  is a unit vector in the laboratory  $z$ -direction and  $\hat{e}_\alpha$  is a unit vector in the local coordinate system of the tails. Fig. 7 shows order parameters for the different DMSO concentrations considered in this work. Here we see that at low DMSO concentrations, there is little change in the structure

**FIGURE 7** Order parameter  $S_{CD}$  for phospholipid tails at 350 K. Pure bilayer (solid line), DMSO-A (dotted line), DMSO-B (dashed line), DMSO-C (dot-dashed line), and DMSO-D (solid bold). The circles are the results from the simulation work by Smodyrev and Berkowitz (1999) at 323 K, and squares are experimental NMR measurements (Petrache et al., 2000) at 353 K.

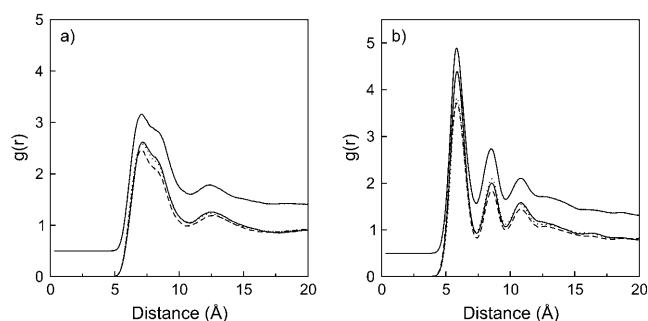


FIGURE 8 (a) Nitrogen-nitrogen and (b) phosphorus-phosphorus radial distribution functions for the DPPC/water/DMSO system at 350 K. DMSO-A (solid line), DMSO-B (dotted line), and DMSO-C (dashed line). Displaced curves are the RDFs for the lipid bilayer system without DMSO.

of the lipid tails. At 10 mol % DMSO and 350 K, the tail order parameters are slightly lower than those of aqueous bilayers because a significant amount of DMSO is found inside the bilayer. However, for the DPPC system in pure DMSO, our results indicate a large decrease in the tail order parameter; this is a consequence of the large amount of DMSO in the bilayer region, which also causes greater disorder among the tails. Comparison of our results to those from Smondyrev and Berkowitz (1999) for a system in pure DMSO reveal that the order parameter shows significant magnitude differences, but appears to follow similar trends. It should again be noted that the results from Smondyrev and Berkowitz are based on a different force field and were obtained at 323 K.

To gain some insights into the equilibrium structure of the lipid bilayer, we have analyzed the spatial distribution of the various groups/molecules in the system through various radial distribution functions (RDF). Figs. 8–11 show the radial distribution function for various groups and molecules at different DMSO concentrations. Fig. 8 shows the radial distribution function for the lipid headgroups (nitrogen-nitrogen and phosphorus-phosphorus); the features of these distribution functions follow closely those seen for the lipid bilayer in the absence of DMSO (*displaced curves* in Fig. 8). The lipid headgroups are well-solvated by water molecules and, as seen in Fig. 9, the overall structure of water around the lipid headgroups is unchanged. From the radial

distribution functions between the lipid polar groups and DMSO (Figs. 10 and 11), one sees that DMSO is more concentrated around the choline group. Two factors are responsible for this effect: 1), electrostatic interactions between the oxygen from DMSO, which is negatively charged, and the nitrogen in the choline group, with its net positive charge; and 2), the extension of the choline group into the aqueous region, since DMSO favors either the aqueous region or the aliphatic part of the bilayer. The radial distribution functions reflect the unfavorable interaction of DMSO with either the lipid phosphate or ester groups. The various radial distribution functions show that there are few DMSO molecules around either the phosphate or the carbonyl groups. Integration of the radial distribution functions support this argument and indicate that, on average, one DMSO molecule is found at a distance of  $\sim 9$  Å, which is much greater than the first minimum of all radial distribution functions. It is interesting to note that the relative intensity of the radial distribution functions in Figs. 10 and 11 decreases with increasing DMSO concentration; this results from the hydrophobic effect discussed earlier. At higher DMSO concentrations, DMSO molecules are depleted from the aqueous region and concentrate near the bilayer tails.

Table 3 compiles the solvation of the polar headgroups. The number of molecules in the first solvation shell around the choline group is determined by counting all water molecules within a distance given by the first minimum in the RDF shown in Fig. 9 *a*. The hydration number for the phosphate and carbonyl groups is determined from geometric criteria that define a hydrogen bond (Brady and Schmidt, 1993). The results in Table 3 indicate that DMSO has a slight effect on the overall solvation of the polar headgroups, as only a small decrease in the number of water molecules is observed. Based on x-ray diffraction and differential scanning calorimetry measurements of lipid bilayers at various DMSO concentrations (Gordeliy et al., 1998; Kiselev et al., 1999; Tristram-Nagle et al., 1998), it has been suggested that DMSO displaces water molecules from the surface by an induced dehydration of the bilayer. Our results have already shown that DMSO does not favor interactions with the lipid headgroups, and DMSO does not replace water molecules bound to the polar headgroups.

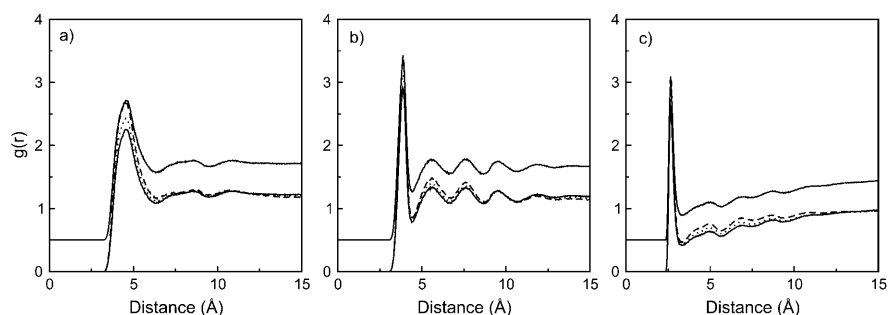


FIGURE 9 Structure of the binding of water molecules to the lipid headgroups at 350 K. The RDFs correspond to water interacting with (a) lipid nitrogen, (b) lipid phosphorus, and (c) lipid carbonyl oxygen. DMSO-A (solid line), DMSO-B (dotted line), and DMSO-C (dashed line). Displaced curves are the RDFs for the lipid bilayer system without DMSO.

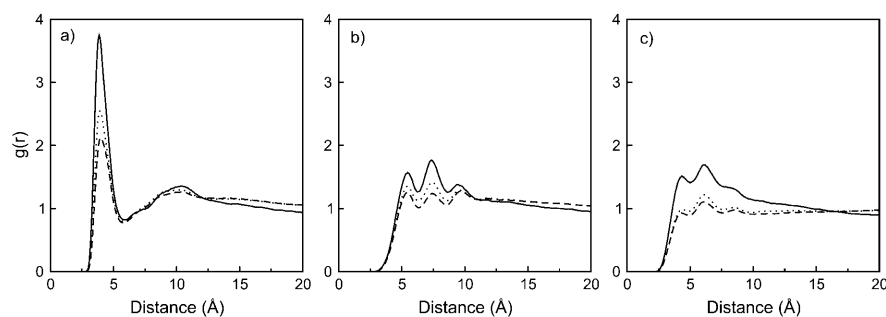


FIGURE 10 Structure of the binding of DMSO molecules to the lipid headgroups at 350 K. The RDFs correspond to DMSO oxygen interacting with (a) lipid nitrogen, (b) lipid phosphorus, and (c) lipid carbonyl oxygen. DMSO-A (solid line), DMSO-B (dotted line), and DMSO-C (dashed line).

We propose that the dehydration induced by DMSO is a consequence of the competition for water molecules between DMSO and the lipid polar groups. It is known that, because of its dipole moment, DMSO hydrogen-bonds to water molecules more strongly than water hydrogen-bonds to itself (Martin and Hauthal, 1971; Shashkov et al., 1999), and in this case, also to the lipid headgroups. This process causes DMSO to pull water molecules away from the bilayer interface to the aqueous region, since DMSO exhibits net repulsive interactions with the phosphate and ester headgroups. The strong binding of DMSO to water molecules modifies the aqueous environment by making water molecules less accessible to the bilayer surface. The changes in the structure and properties of lipid bilayers in the presence of DMSO have been attributed to a strong interaction of DMSO with the bilayer surface (Chang and Dea, 2001; Gordeliy et al., 1998); our results also reveal changes in the structure and properties of the bilayer, but these changes are a consequence of an indirect interaction (induced dehydration) of DMSO with the bilayer surface and a direct interaction with the inner bilayer region (as opposed to a strong interaction of DMSO with the bilayer surface, the actual interaction of DMSO with the surface is minimal). The effect of DMSO on the properties and structure of lipid bilayers appears to be caused by changes in the aqueous phase and a concentration of DMSO in the bilayer phase. Our results are supported by the recent experimental study by Kiselev and co-workers (1999) of DPPC/water/DMSO systems using diffraction, scattering, and calorimetry methods; these authors concluded that at DMSO concen-

trations <30 mol %, DMSO molecules do not concentrate around the polar headgroups or their vicinity, but they remain in the aqueous region and induce the dehydration of the lipid headgroups.

We now turn our attention to several transport properties of the lipid bilayer systems, in particular the rate of diffusion of the lipid headgroup, of water, and of DMSO molecules. Fig. 12 *a* shows the mean-squared displacement of the phosphorus atom of the lipid headgroup at 350 K and 10 mol % DMSO; at short times, the motion of the headgroup is perpendicular to the interfaces, and lateral at long times (because the phosphorus atom is the heaviest, it is representative of the diffusion of the lipid headgroup). This behavior is similar to that observed in the pure bilayer system. Fig. 12 *b* shows the mean-squared displacement of DMSO; here it is seen that the diffusion of DMSO occurs predominantly along the plane of the bilayer surface (*x,y*-plane). Diffusion coefficients *D* can be calculated from the mean-square displacement by

$$D = \lim_{t \rightarrow \infty} \frac{\langle [r(t) - r(0)]^2 \rangle}{2dt}, \quad (5)$$

where *r*(*t*) is the position vector at time *t*, the brackets denote an ensemble average, and *d* = 2 for two-dimensional diffusion. Table 4 shows the calculated diffusion coefficients for the various DMSO concentrations considered here. The long-time diffusion coefficients for the lipids are in good agreement with previously calculated values (Sum et al., 2003) and experimental results (Kuo and Wade, 1979; Vaz et al., 1985) for pure bilayers. Note, however, that the length

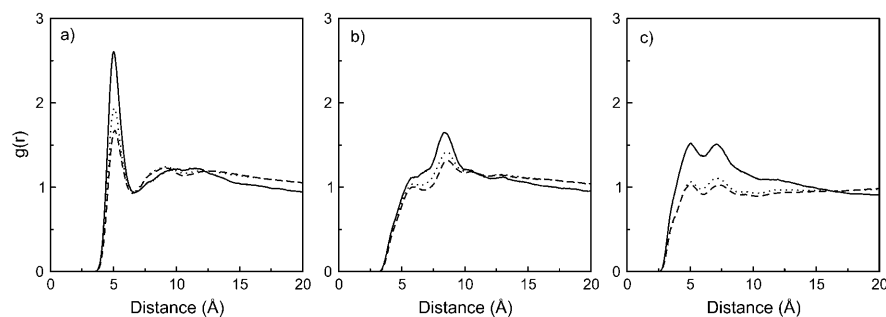


FIGURE 11 Structure of the binding of DMSO molecules to the lipid headgroups at 350 K. The RDFs correspond to DMSO sulfur interacting with (a) lipid nitrogen, (b) lipid phosphorus, and (c) lipid carbonyl oxygen. DMSO-A (solid line), DMSO-B (dotted line), and DMSO-C (dashed line).

**TABLE 3** Average number of water molecules in first solvation shell for choline (N) and average hydration number for phosphate (P) and carbonyl oxygens (Oc) for the lipid headgroup in the ternary DPPC/water/DMSO system

System	<i>T</i> (K)	Choline	Phosphate	Carbonyl oxygen*
Pure	350	19.38	4.12	1.22
DMSO-A	350	18.74	4.06	1.21
DMSO-B	325	19.26	4.09	1.24
	350	18.66	4.11	1.23
	400	18.08	4.01	1.23
DMSO-C	350	17.97	3.97	1.21

\*Mean value between the two carbonyl oxygens.

of our simulations is barely sufficient to attain the diffusive regime for the lipids and the uncertainty of our predictions for  $D_{\text{lipid}}$  is relatively large. DMSO molecules diffuse relatively unhindered; the simulated diffusion coefficients at

**TABLE 4** Long-time two-dimensional diffusion coefficients for the phosphorus atom in the lipid headgroup, DMSO, and water molecules in the lipid bilayer system

System	<i>T</i> (K)	$D_{\text{lipid}}$	$D_{\text{DMSO}}$	$D_{\text{water}}$
Pure	350	$0.33 \pm 0.1$	—	$45.5 \pm 2.0$
DMSO-A	350	$0.29 \pm 0.1$	$8.9 \pm 0.2$	$34.5 \pm 2.0$
DMSO-B	325	$0.19 \pm 0.1$	$6.1 \pm 0.2$	$15.8 \pm 2.0$
	350	$0.26 \pm 0.1$	$8.5 \pm 0.2$	$25.6 \pm 2.0$
	400	$1.00 \pm 0.1$	$16.5 \pm 0.2$	$54.7 \pm 2.0$
DMSO-C	350	$0.40 \pm 0.1$	$10.0 \pm 0.2$	$22.3 \pm 2.0$
Experimental		$0.095^*/0.125^\dagger$	$9.5^\ddagger/6.1^\S$	$64.6^\P$

All values reported as  $D \times 10^6 \text{ cm}^2/\text{s}$ .

\*Pulsed NMR measurement for pure bilayer at 323 K (Kuo and Wade, 1979).

†Fluorescence recovery after photobleaching for pure bilayer at 323 K (Vaz et al., 1985).

‡Liquid DMSO at 298 K (Vishnyakov et al., 2001).

§(1:3) DMSO:Water mixture at 303 K (Packer and Tomlinson, 1971).

¶NMR measurement at 358 K (Ekdawi-Sever et al., 2003).

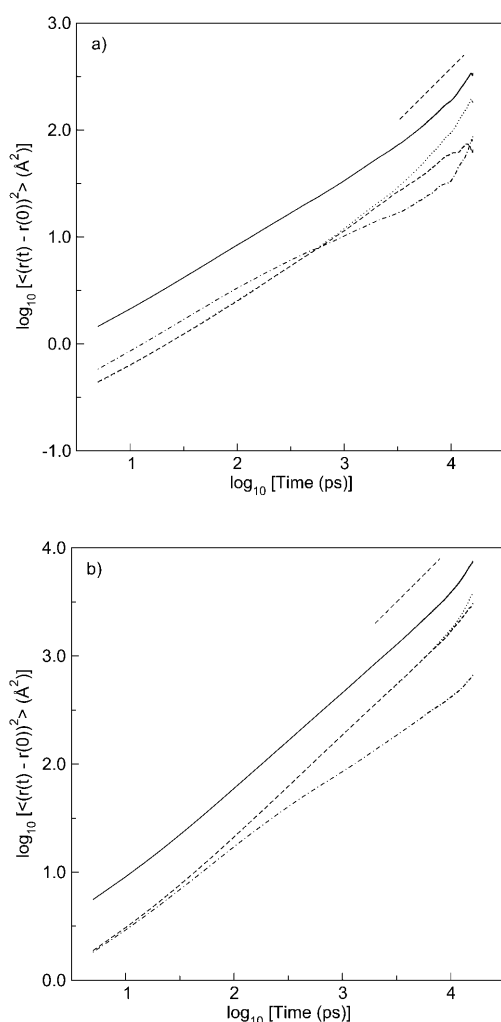


**FIGURE 12** Mean-squared displacement for (a) phosphorus atom in the lipid headgroup and (b) DMSO molecules in the DMSO-C system at 350 K. Solid, dashed, dotted, and dot-dashed lines correspond to *total*, *x*, *y*, and *z*-components, respectively, of the mean-squared displacement. Short dash-line has slope of unity.

350 K are in the range  $D_{\text{DMSO}} = 8.5\text{--}10.0 \times 10^{-6} \text{ cm}^2/\text{s}$ , which compares favorably with measured values for liquid DMSO at 298 K,  $D_{\text{DMSO}} = 9.5 \times 10^{-6} \text{ cm}^2/\text{s}$  (Vishnyakov et al., 2001), and in 1:3 DMSO:water mixtures at 303 K,  $D_{\text{DMSO}} = 6.1 \times 10^{-6} \text{ cm}^2/\text{s}$  (Packer and Tomlinson, 1971). In contrast, the diffusion coefficient of water in the bilayer systems in the presence of DMSO is significantly lower than in its absence. At the highest DMSO concentration considered in this work (10 mol %) and 350 K, the diffusion coefficient of water is  $D_{\text{water}} = 22.3 \pm 2.0 \times 10^{-6} \text{ cm}^2/\text{s}$ , which is half the value in the DPPC/water system. As explained above, we attribute the decrease in mobility of water to the hydrogen-bonding between water and DMSO; DMSO is heavier than water and its diffusion coefficient is approximately one order of magnitude smaller.

## CONCLUSIONS

We have presented a systematic simulation study of the ternary system DPPC/water/DMSO at various DMSO concentrations and several temperatures. DMSO exhibits unique characteristics; it is small in size and has a dual, hydrophilic and hydrophobic character. The favorable binding of water molecules to DMSO induces a dehydration of the lipid bilayer, which is reflected in the decrease of solvation of the polar headgroups. DMSO has the ability to penetrate and diffuse from side to side of the lipid bilayer; this result is seen from the density profiles and the trajectory of DMSO molecules over the course of simulation runs >10 ns. The density profiles show that DMSO can concentrate in the bilayer, mainly in the region adjacent (below or above) the headgroup. However, DMSO is excluded from the lipid headgroups through unfavorable interactions. The concentration of DMSO in the bilayer becomes more pronounced with increasing temperature; this behavior is a consequence of an underlying change in character from hydrophilic to hydrophobic. At higher temperatures, the binding of DMSO



with water becomes weaker and it favors interactions with the lipid bilayer; this increase in DMSO concentration in the bilayer helps explain the known toxicity that occurs at higher temperatures. The crossing of DMSO molecules through the bilayer interface is an activated process; that is, a large energy barrier (breaking of hydrogen-bond between DMSO and water) must be overcome for DMSO molecules in the aqueous region to penetrate the bilayer; once in the bilayer, DMSO molecules can diffuse unhindered. Our results also show that, even though DMSO interacts strongly with water, there is no evidence of any water molecule penetrating the bilayer; water molecules bound to DMSO in the aqueous phase must be released in the bilayer crossing process. At 10 mol % DMSO, a significant amount of DMSO molecules diffuse through the interface and accumulate in the bilayer. For the DPPC system with pure DMSO, the concentration of DMSO is considerably larger. DMSO has a molecular volume greater than water, and its penetration through the interface induces significant expansion of the spacing between the lipid headgroups, which is reflected in the large increase in the area per headgroup of the lipids. Although some of these observations disagree with an earlier simulation study, our findings are consistent with recent experimental data.

We are very grateful to the U.S. National Science Foundation (CTS-0218357) and Defense Advanced Research Projects Agency (DARPA) for the financial support of this project.

## REFERENCES

- Allen, M. P., and D. J. Tildesley. 1987. *Computer Simulation of Liquids*. Clarendon Press, Oxford, UK.
- Anchordoguy, T. J., J. F. Carpenter, J. H. Crowe, and L. M. Crowe. 1992. Temperature-dependent perturbation of phospholipid bilayers by dimethylsulfoxide. *Biochim. Biophys. Acta*. 1104:117–122.
- Anchordoguy, T. J., C. A. Cecchini, J. H. Crowe, and L. M. Crowe. 1991. Insights into the cryoprotective mechanism of dimethyl sulfoxide for phospholipid bilayers. *Cryobiology*. 28:467–473.
- Berendsen, H. J. C., J. R. Grigera, and T. P. Straatsma. 1987. The missing term in effective pair potentials. *J. Phys. Chem.* 91:6269–6271.
- Berendsen, H. J. C., J. P. M. Postma, W. F. van Gunsteren, A. DiNola, and J. R. Haak. 1984. Molecular dynamics with coupling to an external heat bath. *J. Chem. Phys.* 81:3684–3690.
- Bordat, P., J. Sacristan, D. Reith, S. Girard, A. Glättli, and F. Müller-Plathe. 2003. An improved dimethyl sulfoxide force field for molecular dynamics simulations. *Chem. Phys. Lett.* 374:201–205.
- Brady, J. W., and R. K. Schmidt. 1993. The role of hydrogen bonding in carbohydrates: molecular dynamics simulations of maltose in aqueous solution. *J. Phys. Chem.* 97:958–966.
- Chang, H. H., and P. K. Dea. 2001. Insights into the dynamics of DMSO in phosphatidylcholine bilayers. *Biophys. Chem.* 94:33–40.
- Ekdawi-Sever, N. C., J. J. de Pablo, E. Feick, and E. von Meerwall. 2003. Diffusion of sucrose and  $\alpha,\alpha$ -trehalose in aqueous solutions. *J. Phys. Chem. A*. 107:936–943.
- Essman, U., L. Perera, M. L. Berkowitz, T. Darden, H. Lee, and L. G. Pedersen. 1995. A smooth particle mesh Ewald method. *J. Chem. Phys.* 103:8577–8593.
- Faraldo-Gómez, J. D., G. R. Smith, and M. S. P. Sansom. 2002. Setting up and optimization of membrane protein simulations. *Eur. Biophys. J.* 31:217–227.
- Freshney, R. 1987. *Culture of Animal Cells: A Manual of Basic Technique*. Alan R. Liss, Inc., New York.
- Gordeliy, V. I., M. A. Kiselev, P. Lesieur, and J. Teixeira. 1998. Lipid membranes structure and interactions in dimethyl sulfoxide/water mixtures. *Biophys. J.* 75:2343–2351.
- Jacob, S. W., and R. Herschler. 1986. Pharmacology of DMSO. *Cryobiology*. 24:14–27.
- Kiselev, M. A., P. Lesieur, A. M. Kiselev, C. Grabielle-Madelmond, and M. Ollivon. 1999. DMSO-induced dehydration of DPPC membranes studied by x-ray diffraction, small-angle neutron scattering, and calorimetry. *J. Alloys Comp.* 286:195–202.
- Kuo, A.-L., and C. Wade. 1979. Lipid lateral diffusion by pulsed nuclear magnetic resonance. *Biochemistry*. 18:2300–2308.
- Martin, D., and H. G. Hauthal. 1971. *Dimethyl-Sulphoxide*. Van Nostrand Reinhold, New York.
- Nath, S. K., B. J. Banaszak, and J. J. de Pablo. 2001. A new united atom force field for  $\alpha$ -olefins. *J. Chem. Phys.* 114:3612–3616.
- Nath, S. K., and J. J. de Pablo. 2000. Simulation of vapour-liquid equilibria for branched alkanes. *Mol. Phys.* 98:231–238.
- Nath, S. K., F. A. Escobedo, and J. J. de Pablo. 1998. On the simulation of vapor-liquid equilibria for alkanes. *J. Chem. Phys.* 108:9905–9911.
- Nina, M., and T. Simonson. 2002. Molecular dynamics of the tRNA<sup>ala</sup> acceptor stem: Comparison between continuum reaction field and particle-mesh Ewald electrostatic treatments. *J. Phys. Chem. B*. 106:3696–3705.
- Norberg, J., and L. Nilsson. 2000. On the truncation of long-range electrostatic interactions in DNA. *Biophys. J.* 79:1537–1553.
- Paci, E., and M. Marchi. 1994. Membrane crossing by a polar molecule: a molecular dynamics simulation. *Mol. Simul.* 14:1–10.
- Packer, K. J., and D. J. Tomlinson. 1971. Nuclear spin relaxation and self-diffusion in the binary system, dimethyl sulfoxide (DMSO) + water. *J. Trans. Faraday Soc.* 67:1302–1314.
- Patra, M., M. Karttunen, M. T. Hyvönen, E. Falck, P. Lindqvist, and I. Vattulainen. 2003. Molecular dynamics simulations of lipid bilayers: major artifacts due to truncating electrostatic interactions. *Biophys. J.* 84:3636–3645.
- Petrache, H. I., S. W. Dodd, and M. F. Brown. 2000. Area per lipid and acyl length distributions in fluid phosphatidylcholines determined by <sup>2</sup>H NMR spectroscopy. *Biophys. J.* 79:3172–3192.
- Shashkov, S. N., M. A. Kiselev, S. N. Tioutiinnikov, A. M. Kiselev, and P. Lesieur. 1999. The study of DMSO/water and DPPC/DMSO/water system by means of the x-ray, neutron small-angle scattering, calorimetry and IR spectroscopy. *Phys. B*. 271:184–191.
- Smondryev, A. M., and M. L. Berkowitz. 1999. Molecular dynamics simulation of DPPC bilayer in DMSO. *Biophys. J.* 76:2472–2478.
- Sum, A. K., R. Faller, and J. J. de Pablo. 2003. Molecular simulation study of phospholipid bilayers and insights of the interactions with disaccharides. *Biophys. J.* 85:2830–2844.
- Tieleman, D. P., S. J. Marrink, and H. J. C. Berendsen. 1997. A computer perspective of membranes: molecular dynamics studies of lipid bilayer systems. *Biochim. Biophys. Acta Rev. Biomem.* 1331:235–270.
- Tobias, D. J. 2001. Electrostatics calculations: recent methodological advances and applications to membranes. *Curr. Opin. Struct. Biol.* 11:253–261.
- Tristam-Nagle, S., T. Moore, H. I. Petrache, and J. F. Nagle. 1998. DMSO produces a new subgel phase in DPPC: DSC and x-ray diffraction study. *Biochim. Biophys. Acta*. 1369:19–33.
- van Gunsteren, W. F., S. R. Billeter, A. A. Eising, P. H. Hünenberger, P. Krüger, A. E. Mark, W. R. P. Scott, and I. G. Tironi. 1996. *Biomolecular Simulation: The GROMOS Manual and User Guide*. Vdf, Zürich, Switzerland.

- Vaz, W. L. C., R. M. Clegg, and D. Hallman. 1985. Translational diffusion of lipids in liquid-crystalline phase phosphatidylcholine multibilayers—a comparison of experiment with theory. *Biochemistry*. 24:781–786.
- Vishnyakov, A., A. P. Lyubartsev, and A. Laaksonen. 2001. Molecular dynamics simulations of dimethyl sulfoxide and dimethyl sulfoxide-water mixture. *J. Phys. Chem. A*. 105:1702–1710.
- Yamashita, Y., K. Kinoshita, and M. Yamazaki. 2000. Low concentration of DMSO stabilizes the bilayer gel phase rather than the interdigitated gel phase in dihexdecylphosphatidylcholine membrane. *Biochim. Biophys. Acta*. 1467:395–405.
- Yu, Z.-W., and P. J. Quinn. 1998. Solvation effects of dimethyl sulphoxide on the structure of phospholipid bilayers. *Biophys. Chem.* 70:35–39.
- Yu, Z.-W., and P. J. Quinn. 2000. The effect of dimethyl sulphoxide on the structure and phase behaviour of palmitoleoylphosphatidylethanolamine. *Biochim. Biophys. Acta*. 1509:440–450.